Supporting Information

Efficient Coupling of Hierarchical V_2O_5@Ni_3S_2 Hybrid Nanoarray for Pseudocapacitors and Hydrogen Production

Xiongwei Zhong[+, a, b], Linfei Zhang[+, b], Jun Tang[b], Jianwei Chai[c], Jincheng Xu[a], Lujie Cao[a, b], Mingyang Yang[a, b], Ming Yang[c], Weiguang Kong[b], Shijie Wang[c], Hua Cheng[b], Zhouguang Lu[b], Chun Cheng[, b], Baomin Xu*[, b], and Hui Pan*[,a]*

[a] *Institute of Applied Physics and Materials Engineering, University of Macau, Macao SAR, China*

[b] *Department of Materials Science and Engineering, Southern University of Science and Technology, Shenzhen, Guangdong Province, 518055, China*

[c] *Institute of Materials Research and Engineering (IMRE), A*STAR (Agency for Science, Technology, and Research), #08-03, 2 Fusionopolis Way, Innovis, Singapore 138634.*

* Corresponding authors. Tel.: +853 88224427;

E-mail address: chengc@sustc.edu.cn (Chun Cheng); xubm@sustc.edu.cn (Baomin Xu); huipan@umac.mo (Hui Pan)

+ These authors contributed equally to this work.

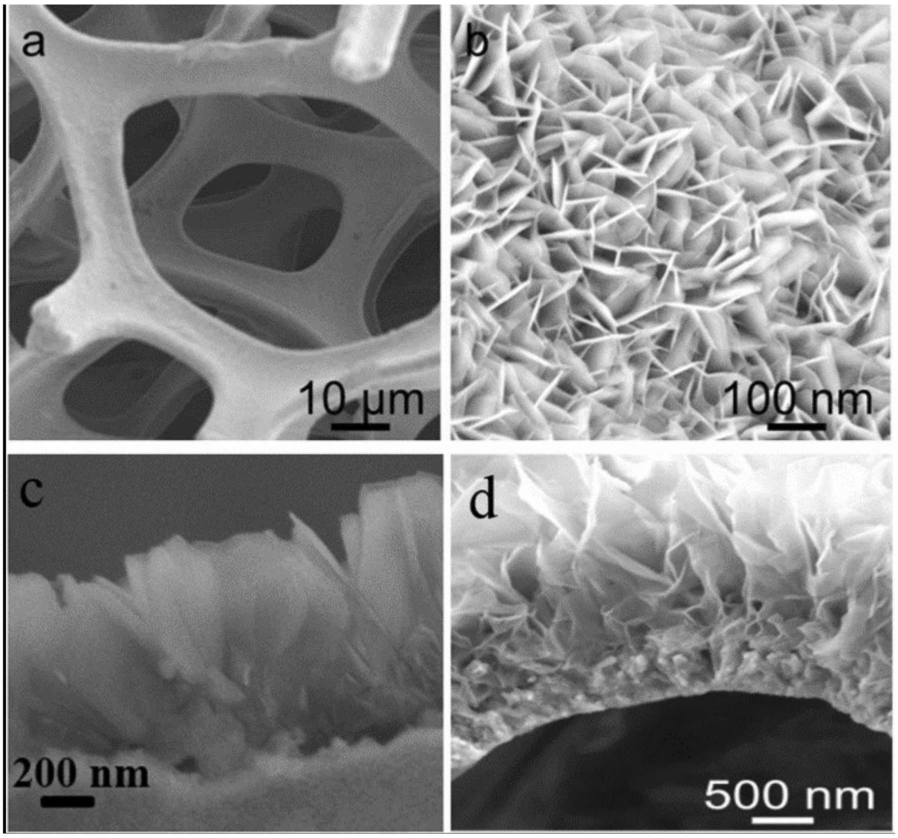

Figure S1. a) The top view, b) high-resolution, c) side view SEM images of a representative Ni_3S_2 nanosheet, respectively. (d) A side view SEM image of V_2O_5@ Ni_3S_2.

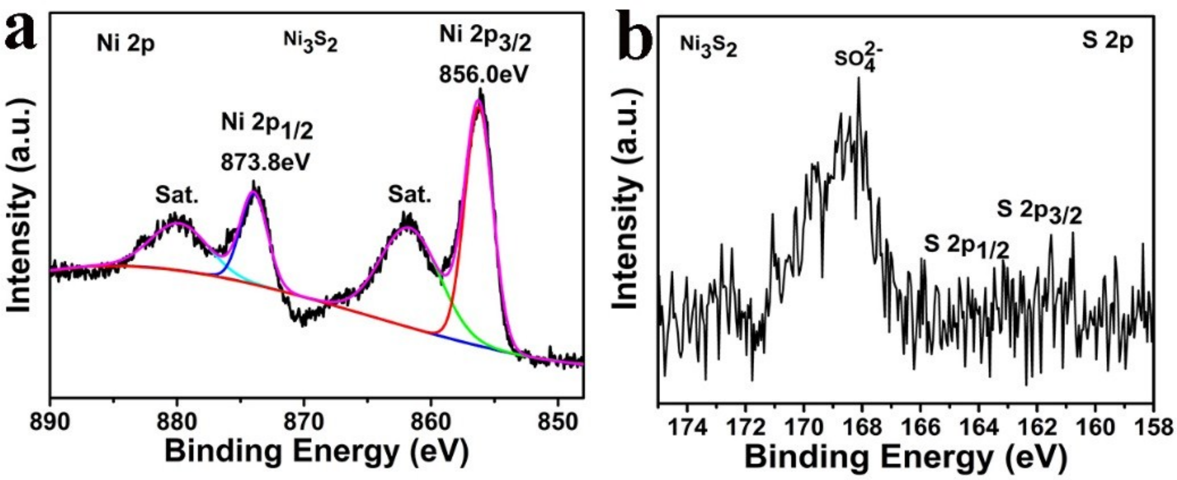

Figure S2. a) Ni 2p and b) S 2p XPS spectral peaks for Ni_3S_2 nanosheet.

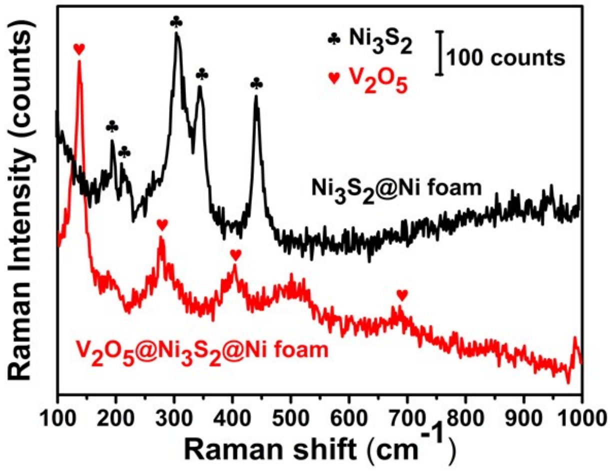

Figure S3. The Raman spectrum of Ni_3S_2 (black) and V_2O_5@Ni_3S_2 (blue) nanosheets.

From Figure S3, the Raman intensity of Ni_3S_2 in the V_2O_5@Ni_3S_2 sample is very low, and only strong V_2O_5 can be detected. These results suggest the V_2O_5 nanosheet completely cover Ni_3S_2 nanosheet.

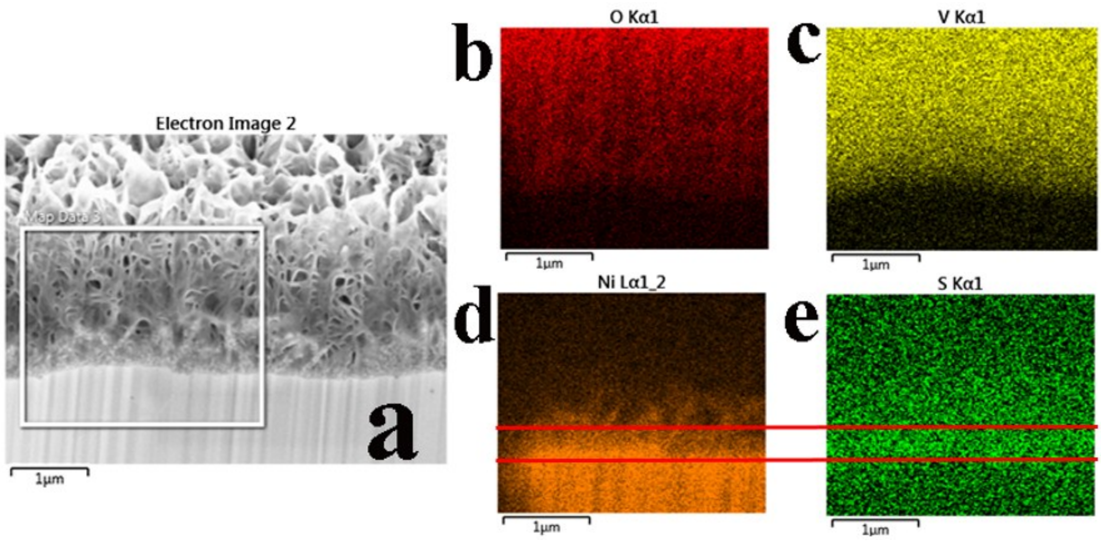

Figure S4. a) The SEM image showing the cross-section of V_2O_5@Ni_3S_2, using the FIB technique. The energy dispersive spectroscopy mapping of b) O, c) V, d) Ni and e) S, and the region correspongding to a).

Figure S4 reveals that V_2O_5 is on the top, Ni_3S_2 in the middle and Ni foam at the bottom. The thicknesses of V_2O_5 and Ni_3S_2 layer are approximate 2 μm and 0.4 μm, respectively. The element dispersive mappings of Ni and S overlapps at the middle region, indicating this layer is Ni_3S_2.

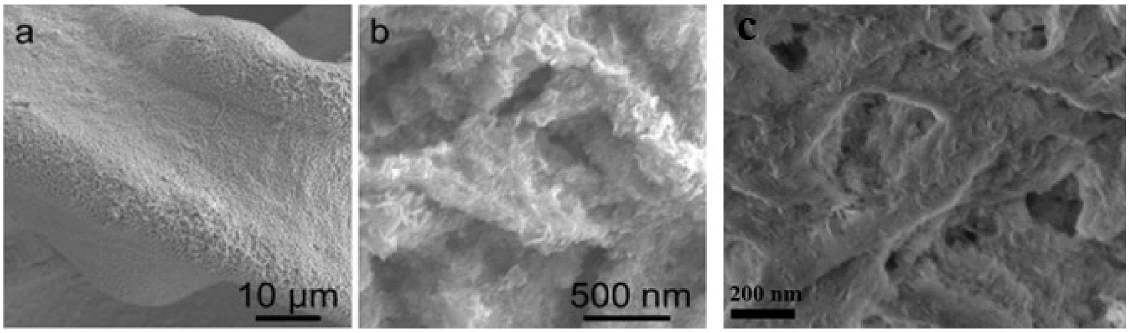

Figure S5. a) A top-view, b) a high-resolution SEM images of V_2O_5@Ni_3S_2 after 1000 galvanostatic charge/discharge (GCD) cycles. c) The SEM image of Ni_3S_2 after 1000 GCD cycles.

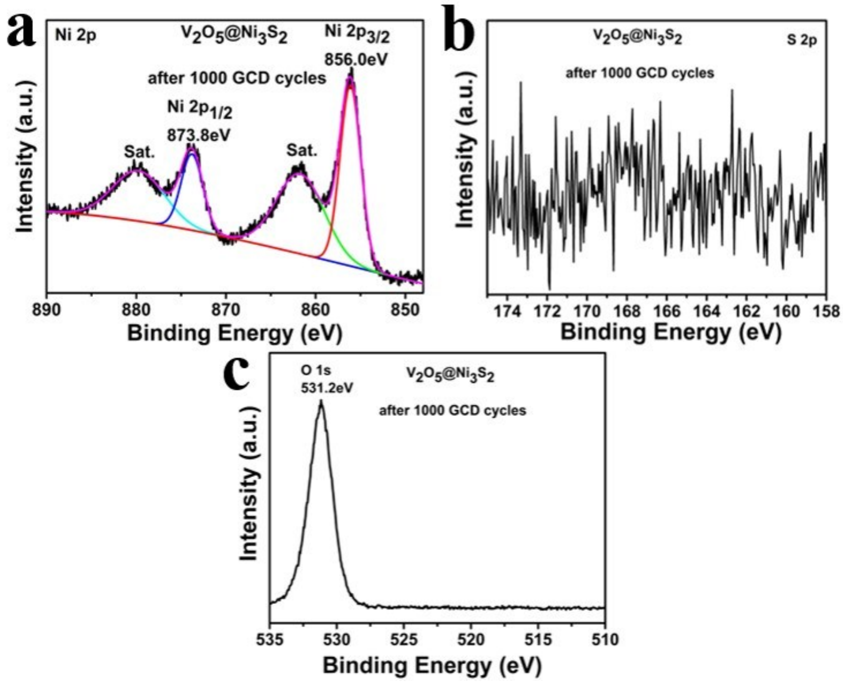

Figure S6. The a) Ni 2p, b) S 2p and c) O 1s XPS spectra of V_2O_5@Ni_3S_2 after 1000 GCD cycles.

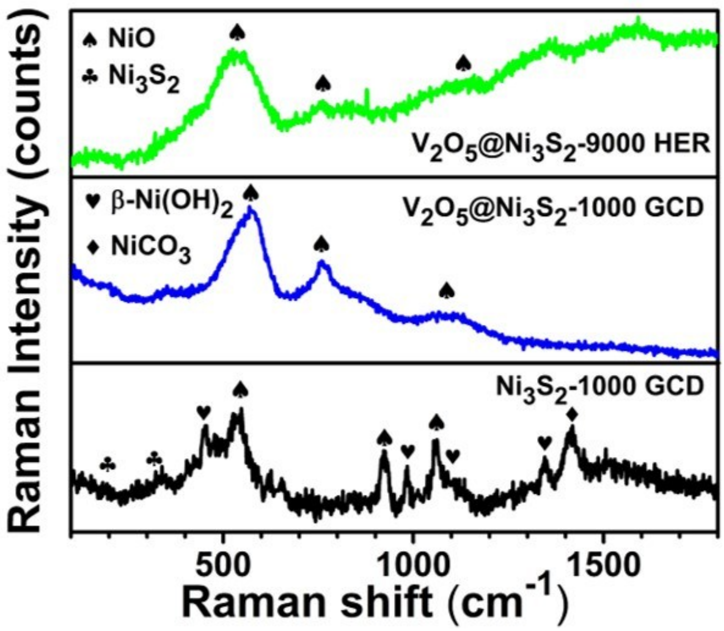

Figure S7. Raman spectra of Ni_3S_2 after 1000 GCD cycles, and V_2O_5@Ni_3S_2 after 1000 GCD cycles and 9000 linear sweep voltammetry (LSV) cycles, respectively.

The Raman spectroscopic investigation was conducted to identify the surface chemical composition of Ni_3S_2 and V_2O_5@Ni_3S_2 after GCD and HER cycles, respectively. For Ni_3S_2 after 1000 GCD cycles, the peak at 545 cm^{-1} was attributed to one-phonon longitudinal optical (LO), the peak at 923 cm^{-1} could be assigned to one-phonon transverse optical and one-phono longitudinal optical mode (TO+LO), and the peak at 1060 cm^{-1} was attributed to two-phono longitudinal optical mode (2LO) mode. In addition, there are four peaks at 453 cm^{-1}, 983 cm^{-1}, 1103 cm^{-1} and 1347 cm^{-1} related to the β-$Ni(OH)_2$ [3-5], two peaks at 196 cm^{-1} and 320 cm^{-1} related to the Ni_3S_2 [6] and one peak at 1416 cm^{-1} corresponded to $NiCO_3$ [7]. It reveals that the V_2O_5 grown on Ni_3S_2 which can be efficiently impeded Ni_3S_2 corrosion and produced to β-$Ni(OH)_2$ and the β-$Ni(OH)_2$ maybe reacted with carbon oxide form air to form $NiCO_3$.

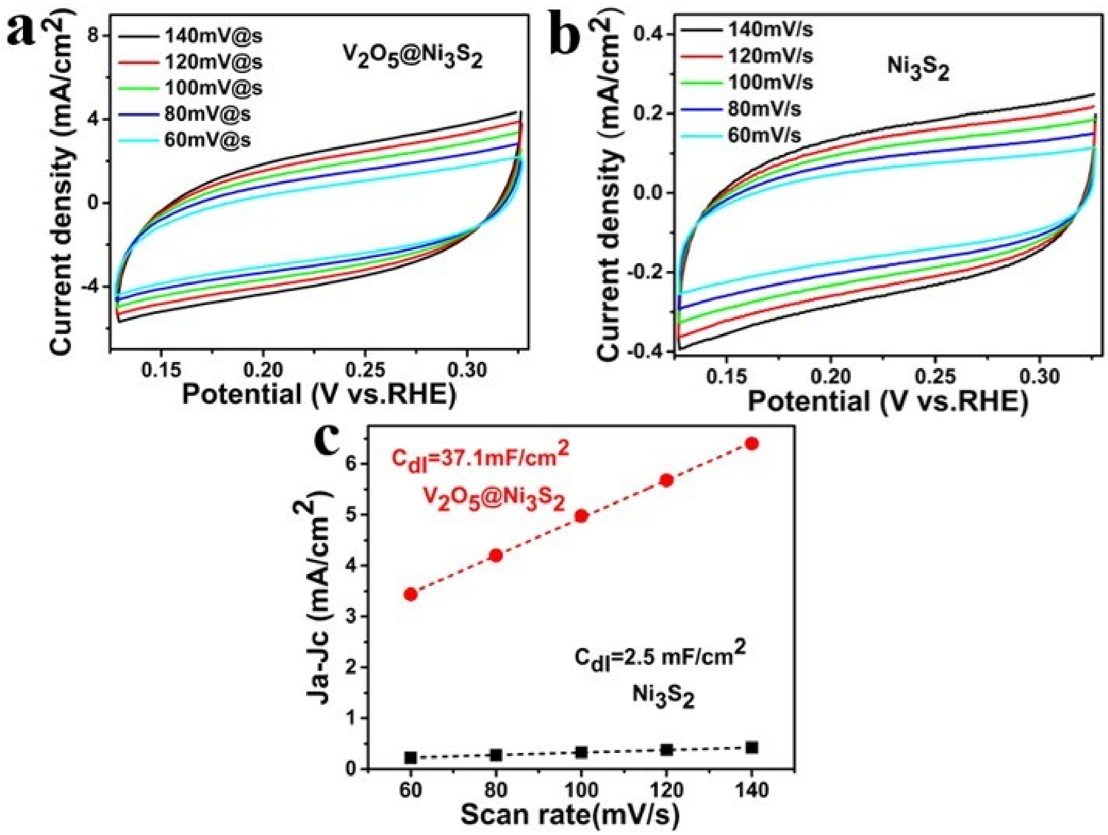

Figure S8. a), b) Cyclic voltammograms (CVs) at different scan rate in the region of 0.13V~0.32 V (vs. RHE) for V_2O_5@Ni_3S_2 and Ni_3S_2, respectively. c) The variation of double-layer charging currents of V_2O_5@Ni_3S_2 and Ni_3S_2 at 0.225 V (vs. RHE) under various scan rates, respectively.

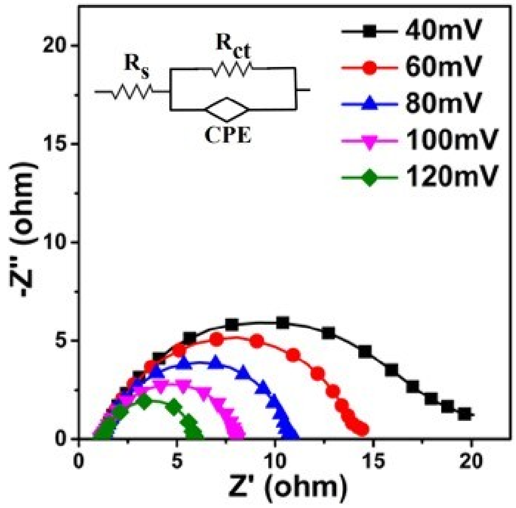

Figure S9. Nyquist plots of $V_2O_5@Ni_3S_2$ at various HER overpotentials.

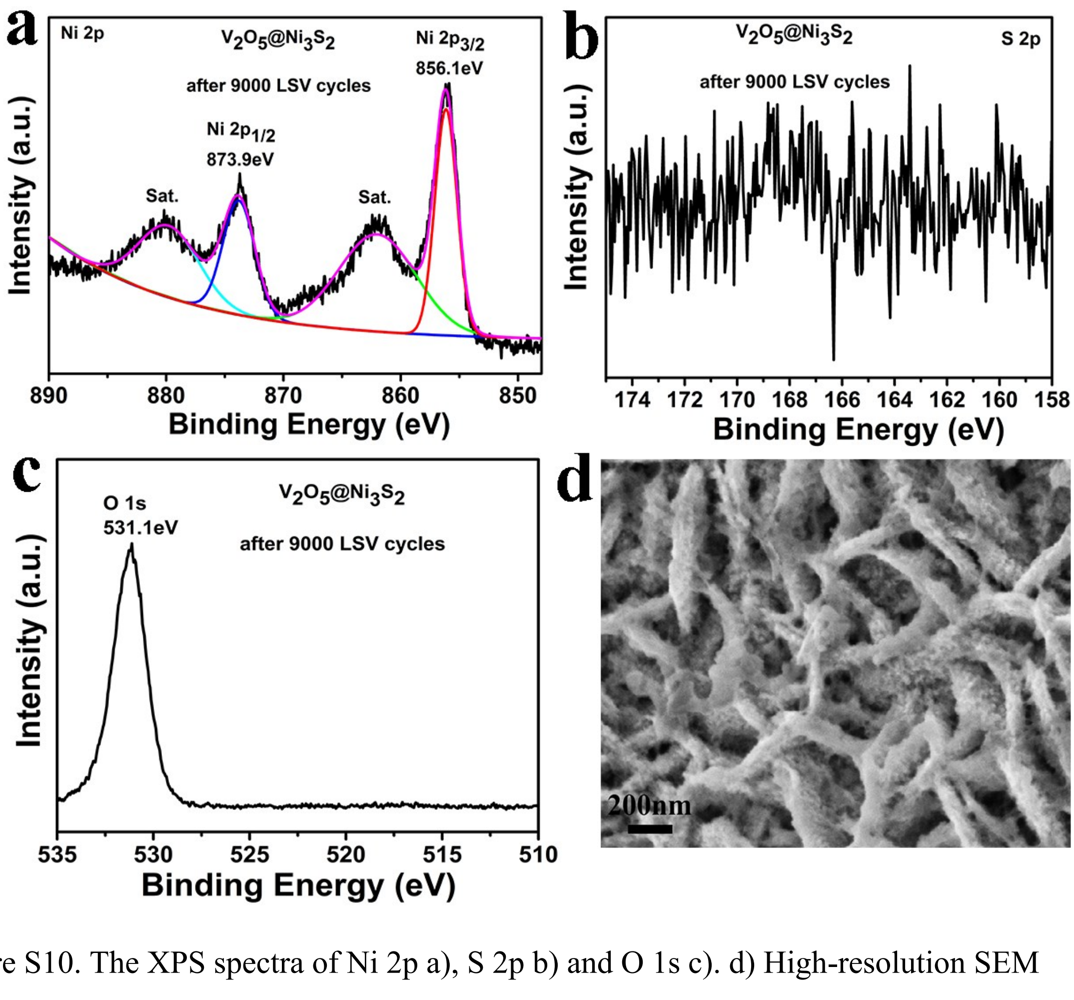

Figure S10. The XPS spectra of Ni 2p a), S 2p b) and O 1s c). d) High-resolution SEM image of $V_2O_5@Ni_3S_2$ after 9000 LSV cycles.

References

1. C. Liu, C. Li, K. Ahmed, Z. Mutlu, C. S. Ozkan and M. Ozkan, *Scientific reports*, 2016, **6**, 29183-29190.
2. S. Wu, K. Hui, K. Hui and K. H. Kim, *Journal of Materials Chemistry A*, 2016, **4**, 9113-9123.
3. H. Li, M. Yu, F. Wang, P. Liu, Y. Liang, J. Xiao, C. Wang, Y. Tong and G. Yang, *Nature communications*, 2013, **4**, 1894-1900.
4. B. Li, M. Ai and Z. Xu, *Chemical Communications*, 2010, **46**, 6267-6269.
5. W. Zhou, X. Cao, Z. Zeng, W. Shi, Y. Zhu, Q. Yan, H. Liu, J. Wang and H. Zhang, *Energy & Environmental Science*, 2013, **6**, 2216-2221.
6. J. Zhang, T. Wang, D. Pohl, B. Rellinghaus, R. Dong, S. Liu, X. Zhuang and X. Feng, *Angew Chem Int Ed Engl*, 2016, **55**, 6702-6707.
7. R. L. Frost, M. L. Weier, W. N. Martens and S. J. Mills, *Neues Jahrbuch für Mineralogie-Abhandlungen: Journal of Mineralogy and Geochemistry*, 2006, **183**, 107-116.